

# Phase Equilibria in Copper(I) Bromide-MBr Systems (M = Li, Na, K)

Alina Wojakowska<sup>a</sup>, Edward Krzyżak<sup>a</sup>, Andrzej Wojakowski<sup>b</sup>, and Marek Wołczyrz<sup>b</sup>

<sup>a</sup> Wrocław Medical University, Department of Inorganic Chemistry, Laboratory of Thermal Analysis, ul. Szewska 38, 50 139 Wrocław, Poland

<sup>b</sup> The W. Trzebiatowski Institute of Low Temperature and Structure Research, Polish Academy of Sciences, ul. Okólna 2, 50 950 Wrocław, Poland

Reprint requests to Dr. habil. A. W.; Fax: +48 71 7840 336;

E-mail: alina.wojakowska@chnorg.am.wroc.pl

Z. Naturforsch. **62a**, 507–512 (2007); received January 16, 2007

*Presented at the EUCHEM Conference on Molten Salts and Ionic Liquids, Hammamet, Tunisia, September 16–22, 2006.*

The phase equilibria of CuBr-LiBr, CuBr-NaBr and CuBr-KBr were studied by difference scanning calorimetry (DSC) and X-ray powder diffraction. Extended solid solutions have been found in CuBr-LiBr, while mutual solid solubility of the components of CuBr-NaBr and CuBr-KBr seems to be negligible. It has been confirmed that  $K_2CuBr_3$  is stable at room temperature.

*Key words:* Phase Diagram; DSC; CuBr; LiBr; NaBr; KBr.

## 1. Introduction

Systems involving copper(I) halides are worth studying in view of their potential high conductivity. By addition of a second component, such as an alkali halide, ionic conducting materials used as solid electrolytes may be produced.

To our knowledge no information on phase equilibria of the system copper(I) bromide-lithium bromide has been reported. Both components are difficult to operate, the former being sensitive to oxidation and the latter to traces of humidity. In this work we present preliminary results on phase equilibria in the CuBr-LiBr system, based on experiments performed under vacuum or in an inert and exsiccated atmosphere.

Phase diagrams of CuBr-NaBr and CuBr-KBr were published by De Cesaris [1] and Biefeld [2]. The CuBr-NaBr system was found to be a simple eutectic system [2]. In the CuBr-KBr system one intermediate compound,  $K_2CuBr_3$ , melting incongruently, was found [1,2]. It was prepared by precipitation from a hot aqueous solution [2,3]. Refined crystal structure data on  $K_2CuBr_3$  were recently published by Hull and Berastegui [3].

The phase diagrams of CuBr-NaBr and CuBr-KBr have been redetermined because of the poor precision of the previous data [1,2]. The phase diagram of CuBr-KBr, presented by De Cesaris [1] in an early

work and based on cooling curves, does not satisfy the Gibbs phase rule. Phase diagrams given by Biefeld [2] for CuBr-NaBr and CuBr-KBr were constructed on the basis of the DTA method, using for each of them only about ten samples with large composition intervals (about 10 mol%). For the eutectic points, the uncertainty of the composition determination was given to be  $\pm 5$  mol%, and that of the temperature determination to be  $\pm 5$  K. Phase diagrams for the CuBr-NaBr and CuBr-KBr systems given in the present work were established by differential scanning calorimetry (DSC), performed on about forty samples for each system. The uncertainty of the composition determination, based on weighing the components, was estimated to be  $\pm 0.1$  mol%, and that of the temperature determination to be  $\pm 1$  K. Compositions of the eutectic and peritectic points were determined by extrapolation of the liquidus curves and by the Tamman triangle method [4] with an uncertainty of 0.5 mol%.

## 2. Experimental

For the DSC measurements a Mettler Toledo DSC 25 measuring cell with an updated STARE<sup>®</sup> software and for the X-ray diffraction experiments a STOE powder diffraction system (in case of the CuBr-LiBr system) or a DRON type diffractometer (in case of the CuBr-NaBr and CuBr-KBr systems) were used.

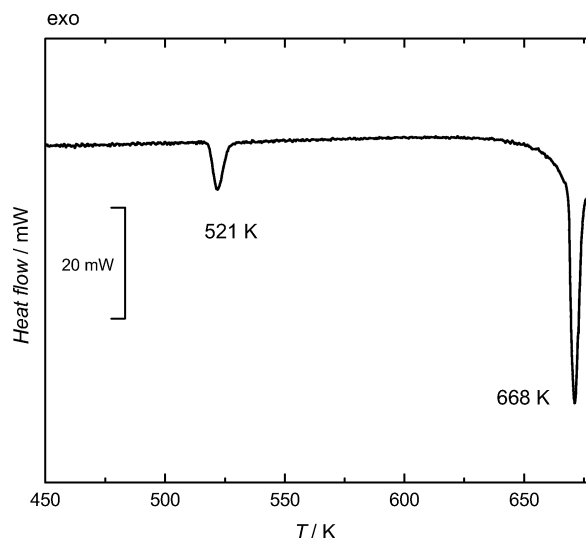


Fig. 1. Example of a DSC curve for  $x_{\text{CuBr}} = 0.504$  showing both formation and decomposition of  $\text{LiCuBr}_2$  at 521 K and 668 K, respectively.

$\text{CuBr}+\text{LiBr}$  mixtures for DSC and X-ray diffraction studies were prepared in a glove box containing argon (Labmaster 130 MBraun). High purity  $\text{CuBr}$  and  $\text{LiBr}$  (both 99.999%, Sigma Aldrich) were used without further purification.  $\text{CuBr}+\text{NaBr}$  and  $\text{CuBr}+\text{KBr}$  mixtures were prepared from high purity  $\text{CuBr}$  (99.999%, Riedel de Haën) and the respective alkali halide (analytical grade, POCH Gliwice), heated beforehand under vacuum to a temperature 50 K above the corresponding melting point and then cooled slowly to room temperature. Appropriate quantities of salts were weighed and introduced into silica ampoules, next sealed under vacuum, heated to melting and homogenized.

Mixtures of salts for DSC experiments were prepared directly in flat, polished bottom ampoules, used afterwards for measurements. Their outer diameter and height (after sealing) were 6 mm and 14 mm, respectively. The composition of samples was taken at intervals of around 2–3 mol% or less.  $\text{CuBr}+\text{NaBr}$  and  $\text{CuBr}+\text{KBr}$  mixtures of a total weight of 20–30 mg were annealed at about 400 K for a few hours before the first heating run was performed at the rate  $5 \text{ K min}^{-1}$ . The total weight of  $\text{CuBr}+\text{LiBr}$  mixtures was generally higher, exceeding occasionally 100 mg. All the homogenized  $\text{CuBr}+\text{LiBr}$  samples were first measured at the heating rate  $1 \text{ K min}^{-1}$  from about 300 K to melting and then cooled back with the same rate. Besides the above runs, a number of heat-

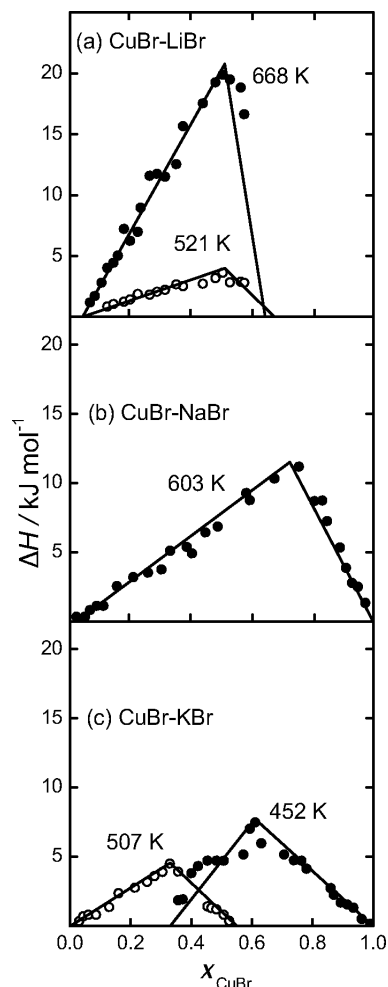


Fig. 2. Tamman triangles for some invariant equilibria: (a) solid state reactions at 521 K and 668 K, respectively, in the  $\text{CuBr-LiBr}$  system; (b) eutectic reaction in the  $\text{CuBr-NaBr}$  system; (c) eutectic and peritectic reaction at 452 K and 507 K, respectively, in the  $\text{CuBr-KBr}$  system.

ing and cooling experiments performed with a rate between  $0.5$  and  $10 \text{ K min}^{-1}$  were carried out during the investigations of the three systems.

### 3. Results and Discussion

The  $\text{CuBr-LiBr}$  system exhibits significant solid solubility of the components, especially  $\text{LiBr}$  in the respective polymorphic modifications of  $\text{CuBr}$ . The solid solubility of  $\text{CuBr}$  in  $\text{LiBr}$  extends to  $x_{\text{CuBr}} \approx 0.07$ . The limits of the solid solubility of  $\text{LiBr}$  in  $\alpha$ -,  $\beta$ - or  $\gamma$ - $\text{CuBr}$  were estimated to be between  $x_{\text{CuBr}} = 0.60$  and  $x_{\text{CuBr}} = 0.65$ , and a range of temperature for the exis-

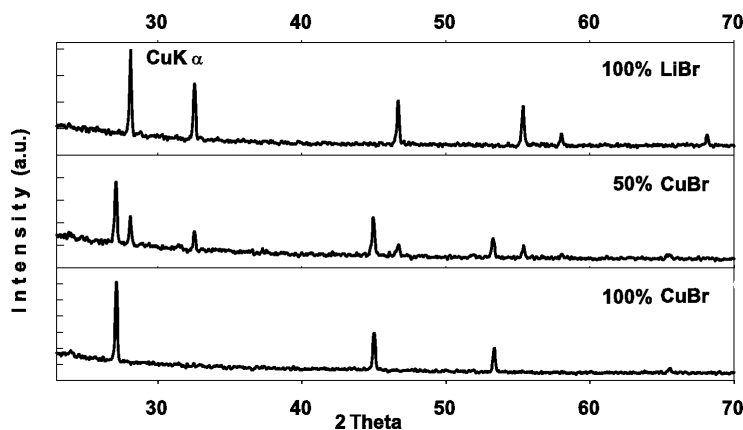


Fig. 3. X-Ray powder diffraction patterns of pure components ( $\gamma$ -CuBr, LiBr) and their 1:1 mixture quenched to room temperature.

tence of high-temperature  $\alpha$  and  $\beta$  superionic phases was found to stretch to 679 K and 645 K, respectively, i. e. 60 K and 95 K below the  $\alpha/\beta$  phase transition in the pure CuBr. Similar wide solid solutions based on CuBr modifications were reported for the CuBr-AgBr system [5]. The extended solid solutions formed in the CuBr-LiBr system are no surprise since the effective radii of  $\text{Cu}^+$  and  $\text{Li}^+$  were often considered as being close to each other, both having a value of about 0.5 Å [6, 7].

Apart from the eutectic reaction at 684 K, clearly marked invariances at 521 K and 668 K were found. They have been interpreted as solid state reactions, resulting in the formation and decomposition of a new phase, stable only between 521 K and 668 K. An example of a DSC curve for  $x_{\text{CuBr}} = 0.504$ , obtained at a heating rate of  $2 \text{ K min}^{-1}$ , is presented in Figure 1. The maximal thermal effect for both reactions occurred at the same composition, about  $x_{\text{CuBr}} = 0.50$  (Fig. 2a), indicating the formula  $\text{LiCuBr}_2$ . This is rather unexpected since 1:1 compounds rarely appear in the copper(I) halide-alkali halide systems [8]. This intermediate phase cannot be quenched to room temperature, as shown by X-ray powder diffraction patterns given in Fig. 3, where only the room temperature  $\gamma$ -CuBr and LiBr phases can be observed.

The phase diagram for the CuBr-NaBr system is of a simple eutectic type (Fig. 4). X-Ray powder diffraction patterns for any mixture, e. g. for  $x_{\text{CuBr}} = 0.333$ , reveal only pure CuBr and NaBr (Fig. 5) lines and the absence of any intermediate compound, stable at room temperature. The eutectic point is situated at 603 K and  $x_{\text{CuBr}} = 0.71$ . The Tamman triangle is shown in Figure 2b. Thermal effects of the eutectic reaction have been observed on DSC thermograms almost in the

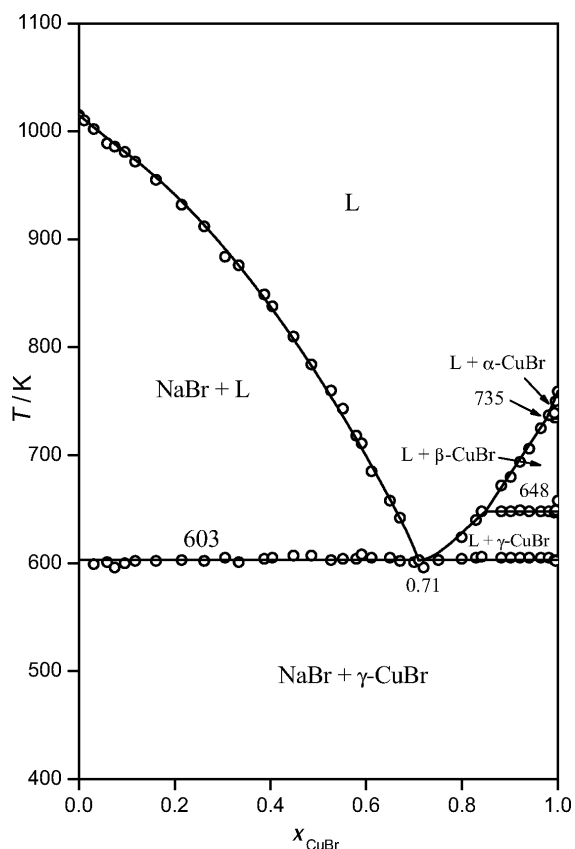


Fig. 4. Phase diagram of the CuBr-NaBr system.

whole range of compositions, indicating that limiting solid solutions at 603 K are negligible, especially on the CuBr side.

Temperatures corresponding to  $\alpha/\beta$  and  $\beta/\gamma$  polymorphic transitions (Fig. 4) display slightly lower values than those in pure CuBr [8]. This may indicate the

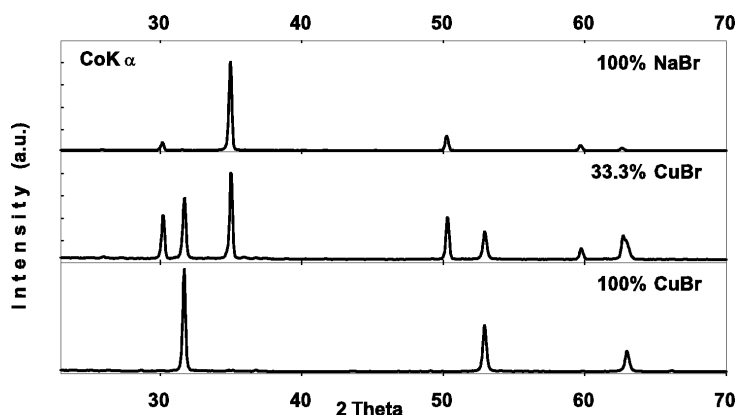


Fig. 5. X-Ray powder diffraction patterns of pure components ( $\gamma$ -CuBr, NaBr) and their 1 : 2 mixture quenched to room temperature.

existence of very narrow solid solutions of NaBr in  $\alpha$ - and  $\beta$ -CuBr (below  $x_{\text{NaBr}} = 0.004$ ). Compositions of the liquid phase for invariances  $\alpha + \text{liquid} = \beta$  and  $\beta + \text{liquid} = \gamma$  were found to be at about  $x_{\text{CuBr}} = 0.98$  and  $x_{\text{CuBr}} = 0.85$ , respectively.

The phase diagram for the CuBr-KBr system obtained in this study is presented in Figure 6. Formation of the compound  $\text{K}_2\text{CuBr}_3$  [1, 2], stable at room temperature, has been confirmed by DSC and X-ray diffraction. The sample containing 33.3 mol% CuBr reveals only an individual X-ray diffraction pattern (Fig. 7), typical of  $\text{M}_2\text{CuX}_3$  phases ( $\text{M} = \text{K}, \text{Rb}; \text{X} = \text{Cl}, \text{Br}$ ) which crystallize in structures with the space group  $Pnma$  [2, 3, 9–13].

$\text{K}_2\text{CuBr}_3$  melts incongruently at 507 K decomposing into KBr and a liquid mixture of the composition  $x_{\text{CuBr}} = 0.56$  (peritectic point). This compound stoichiometry can be evidenced from the DSC curve of a sample with the composition  $x_{\text{CuBr}} = 0.329$  (Fig. 8). This shows only one thermal effect (peritectic reaction at 507 K) while for a sample with higher CuBr content ( $x_{\text{CuBr}} = 0.356$ ) both events, eutectic, at 452 K and peritectic at 507 K, are observed (Fig. 8). The Tamman method shows that the maximum value of the thermal effect at 507 K is given for the mixture with the composition near  $x_{\text{CuBr}} = 0.333$  (Fig. 2c).

It should be noted that in our previous study of the CuBr-KBr system [14] we observed at a temperature very close to that of the eutectic an additional thermal effect until nearly pure KBr. It was ascribed to a polymorphic transition of  $\text{K}_2\text{CuBr}_3$ . However, if samples were annealed at 500 K for about 24 h, the event did not appear on DSC curves. Probably, a similar effect was found in the CuCl-KCl system [15] which resulted in a wrong description of phase equi-

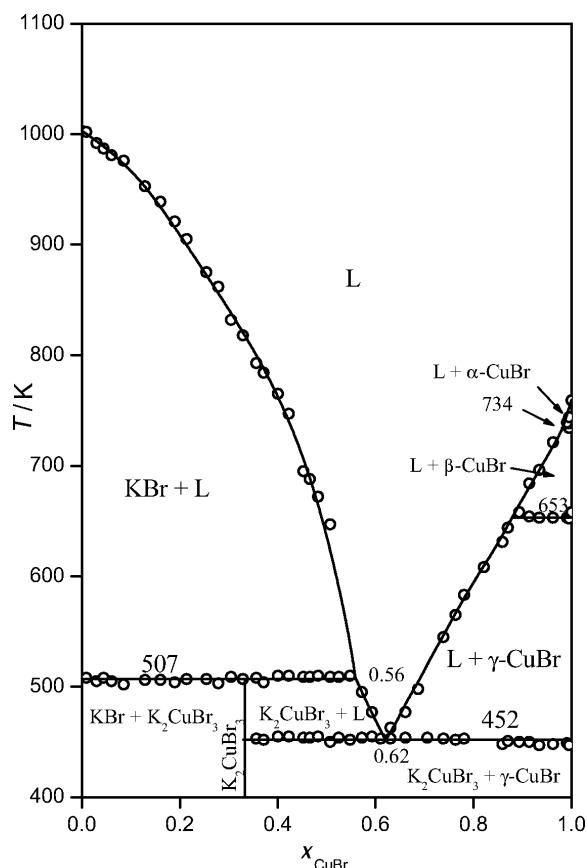


Fig. 6. Phase diagram of the CuBr-KBr system.

libria in this system (non-conforming with the phase rule).

Eutectic reaction at 452 K appears on DSC thermograms for samples having a composition between  $x_{\text{CuBr}} = 0.356$  and  $x_{\text{CuBr}} = 0.995$ . Thermal effects versus composition, presented in Fig. 2c, show the max-

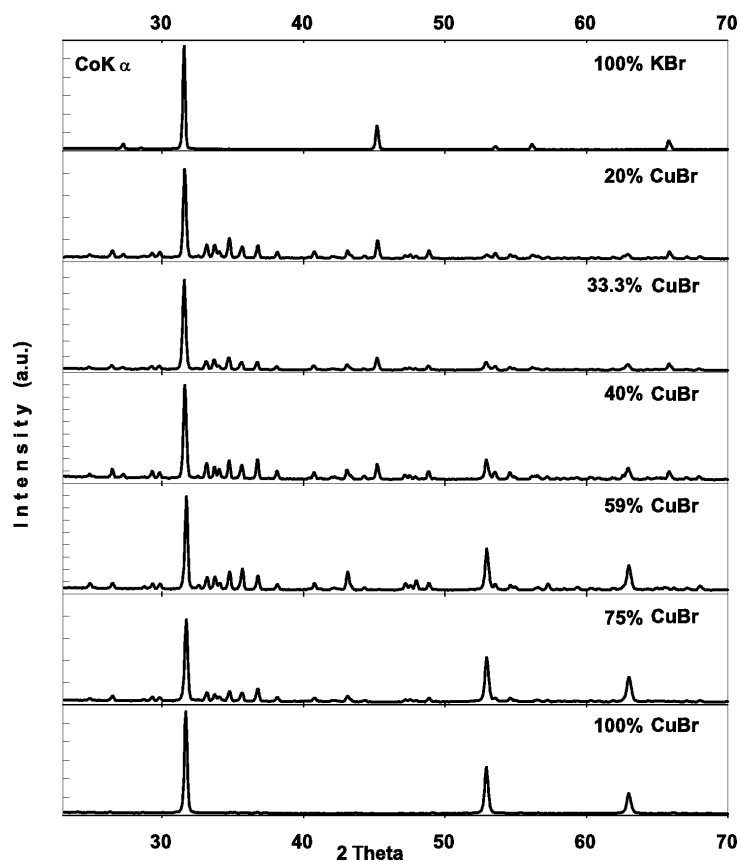


Fig. 7. X-Ray powder diffraction patterns of pure components ( $\gamma$ -CuBr, KBr) and their mixtures quenched to room temperature.

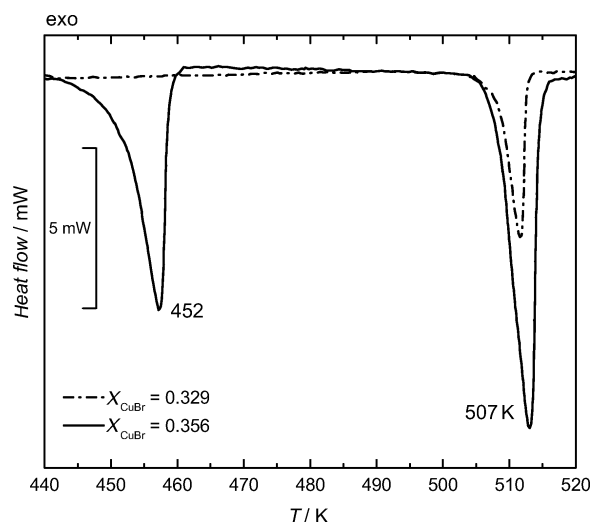


Fig. 8. Examples of DSC curves for  $x_{\text{CuBr}} = 0.329$  and  $x_{\text{CuBr}} = 0.356$ , the former not showing the effect of the eutectic reaction  $\text{K}_2\text{CuBr}_3 + \gamma\text{-CuBr} \leftrightarrow \text{L}$  at 452 K.

imum at  $x_{\text{CuBr}} = 0.62$ , i. e. at the eutectic point, and tend to zero on both the  $\text{K}_2\text{CuBr}_3$  and  $\gamma\text{-CuBr}$  side.

Any solid solution based on  $\gamma\text{-CuBr}$  must be negligible considering that it was possible to grow single crystals of  $\gamma\text{-CuBr}$  from CuBr+KBr molten mixtures [16, 17].

Like in the CuBr-NaBr system, temperatures of thermal events associated with the  $\alpha/\beta$  and  $\beta/\gamma$  polymorphic transitions in the CuBr-KBr system are a little lower than those in pure CuBr [8]. This may indicate a slight solid solubility of KBr in  $\alpha$ - and  $\beta$ -CuBr (below  $x_{\text{KBr}} = 0.005$ ). Thermal effects for invariant transitions  $\alpha + \text{liquid} = \beta$  and  $\beta + \text{liquid} = \gamma$  were observed from nearly pure CuBr to a molten solution with the composition of  $x_{\text{CuBr}} = 0.98$  and  $x_{\text{CuBr}} = 0.88$ , respectively. Absence of solid solutions based on copper(I) bromide in the CuBr-KBr system was predicted by Fang *et al.* [18] as a result of investigations of regularities in the formation of solid solutions in binary monovalent metal halide systems.

Corresponding values of temperatures and phase compositions for invariant (three-phase) equilibria in the CuBr-NaBr and CuBr-KBr systems are gathered in Table 1. Our results, even though they are much more detailed, on the whole agree with those

Reaction	$T/K$	Type	Phase	Composition $x_{\text{CuBr}}$
CuBr-NaBr system				
$\text{NaBr} + \gamma\text{-CuBr} \leftrightarrow \text{L}$	603	eutectic	NaBr $\gamma\text{-CuBr}$ liquid	< 0.025 > 0.996 0.71
$\gamma\text{-CuBr} + \text{L} \leftrightarrow \beta\text{-CuBr}$	648	peritectic	$\gamma\text{-CuBr}$ $\beta\text{-CuBr}$ liquid	1.00 > 0.996 0.85
$\beta\text{-CuBr} + \text{L} \leftrightarrow \alpha\text{-CuBr}$	735	peritectic	$\beta\text{-CuBr}$ $\alpha\text{-CuBr}$ liquid	1.00 1.00 0.98
CuBr-KBr system				
$\gamma\text{-CuBr} + \text{K}_2\text{CuBr}_3 \leftrightarrow \text{L}$	452	eutectic	$\text{K}_2\text{CuBr}_3$ $\gamma\text{-CuBr}$ liquid	0.333 > 0.995 0.62
$\text{KBr} + \text{L} \leftrightarrow \text{K}_2\text{CuBr}_3$	507	peritectic	$\text{K}_2\text{CuBr}_3$ KBr liquid	0.333 < 0.008 0.56
$\gamma\text{-CuBr} + \text{L} \leftrightarrow \beta\text{-CuBr}$	653	peritectic	$\gamma\text{-CuBr}$ $\beta\text{-CuBr}$ liquid	> 0.995 > 0.995 0.88
$\beta\text{-CuBr} + \text{L} \leftrightarrow \alpha\text{-CuBr}$	734	peritectic	$\beta\text{-CuBr}$ $\alpha\text{-CuBr}$ liquid	> 0.995 > 0.995 0.98

Table 1. Invariant three-phase equilibria in the CuBr-NaBr and CuBr-KBr systems.

of Biefeld [2]. They also confirm similarity between bromide and chloride systems: extended solid solutions in both CuCl-LiCl [19] and CuBr-LiBr systems, phase diagrams of the eutectic type in CuCl-NaCl [11] and CuBr-NaBr systems as well as

phase diagrams of CuCl-KCl [11] and CuBr-KBr systems, forming the incongruently melting compounds  $\text{K}_2\text{CuCl}_3$  [11] and  $\text{K}_2\text{CuBr}_3$ , both stable at room temperature and crystallizing in the same type of structure.

- [1] P. De Cesaris, *Atti R. Accad. Lincei* **5**, 749 (1911).  
 [2] R. M. Biefeld, *Mater. Res. Bull.* **10**, 1151 (1975).  
 [3] S. Hull and P. Berastegui, *J. Solid State Chem.* **177**, 3156 (2004).  
 [4] G. Tamman, *Z. Anorg. Chem.* **47**, 289 (1905).  
 [5] M. Saito, H. Takahashi, and S. Tamaki, *Solid State Ionics* **35**, 359 (1989).  
 [6] R. D. Shannon and C. T. Prewitt, *Acta Crystallogr. B* **25**, 925 (1969).  
 [7] P. Dantzer, *J. Phys. Chem.* **85**, 724 (1981).  
 [8] A. Wojakowska and E. Krzyżak, *J. Therm. Anal. Cal.* **83**, 597 (2006).  
 [9] C. Brink and C. H. MacGillavry, *Acta Crystallogr.* **2**, 158 (1948).  
 [10] C. Brink Shoemaker, *Z. Kristallogr.* **137**, 225 (1973).  
 [11] I. V. Vasilkova, I. I. Kozhina, and G. P. Zagolovich, *Vestn. Leningr. Univ., Ser. Fiz. Khim.* **22**, 138 (1978).  
 [12] S. Jagner and G. Helgesson, *Adv. Inorg. Chem.* **37**, 1 (1991).  
 [13] Y. Suenaga, M. Maekawa, T. Kuroda-Sowa, and M. Munakata, *Anal. Sci. (Japan)* **13**, 647 (1997).  
 [14] A. Wojakowska and E. Krzyżak, *Prog. Molten Salts Chem.* **1**, 565 (2000).  
 [15] O. Yamamoto, in: *Fast Ion Transport in Solids*, NATO ASI Series E, Vol. 250 (Eds. B. Scrosati, A. Magistris, C. M. Mori, and G. Mariotto), Kluwer Academic Publishers, Dordrecht 1993, p. 203.  
 [16] Y. Oka, T. Kushida, T. Murahashi, and T. Koda, *J. Phys. Soc. Jpn.* **36**, 245 (1974).  
 [17] C. Schwab and A. Goltzene, *Prog. Cryst. Growth Charact.* **5**, 233 (1982).  
 [18] J. Fang, W. Ding, X. Shen, L. Shi, and N. Chen, *Calphad: Computer Coupling of Phase Diagrams and Thermochemistry* **28**, 9 (2004).  
 [19] E. Korreng, *Neues Jahrb. Mineral. Geol.* **37**, 51 (1914).